Habitable Planet, 2026, 2(2), 413–431

Scilight

Habitable Planet

Journal Homepage: https://www.sciltp.com/journals/hp

INTERNATIONAL ASSOCIATION FOR GONDWANA RESEARCH IAGR

Article

Temporal Resolution Controls on Climate-Signal Preservation in Quaternary Palaeoclimate Records

Monmohan Gogoi* and Diganta Bhuyan

Department of Applied Geology, Dibrugarh University, Dibrugarh 786004, Assam, India

* Correspondence: monmohan017@gmail.com

ABSTRACT

Geological archives provide the primary evidence for reconstructing Quaternary climate variability, yet differences among proxy records are commonly interpreted using broad archive categories. Such classifications can obscure the measurable controls governing the recording and preservation of climate signals. Here, a generalized quantitative framework is developed in which temporal resolution and signal fidelity depend primarily on accumulation rate, sampling integration scale, post-depositional mixing, diffusive smoothing, and ecological response time. Analytical formulations and numerical forward experiments show that increasing effective temporal integration attenuates abrupt events, broadens transition durations, suppresses high-frequency variability, redistributes variance toward longer timescales, and can generate apparent timing offsets between records responding to the same forcing. The framework further shows that uncertainty reduction in multi-record composites is limited when errors are correlated. Representative applications to Greenland ice cores, Chinese speleothems, and North Atlantic marine sediments show how readily available archive metadata can be translated into first-order estimates of effective temporal resolution, climate-signal attenuation, duration inflation, and preserved climatic bandwidth. These results indicate that Quaternary proxy records should be interpreted as filtered representations of climate variability whose characteristics depend on archive-response processes. Explicit integration of effective temporal resolution is essential for cross-archive comparison, proxy synthesis, and model-data evaluation.

ARTICLE INFO

History:

Received: 15 May 2026
Revised: 28 June 2026
Accepted: 27 July 2026
Published: 31 July 2026

Keywords:

quaternary palaeoclimate;
temporal resolution;
proxy archives;
signal preservation;
proxy system models

Citation:

Gogoi, M.; Bhuyan, D. Temporal Resolution Controls on Climate-Signal Preservation in Quaternary Palaeoclimate Records. *Habitable Planet* **2026**, *2*(2), 413–431. https://doi.org/10.63335/j.hp.2026.0046

Research Highlights

- Generalized framework quantifies archive-specific temporal filtering.
- Effective temporal resolution governs climate-signal preservation.
- Representative archives demonstrate practical framework application.
- Temporal bandwidth enables quantitative proxy comparison.
- Framework improves proxy synthesis and model-data integration.

1. Introduction

Natural geological and biological archives provide direct evidence for reconstructing Earth's climate variability beyond the instrumental period and encompass all Quaternary palaeoclimate reconstructions. Marine and lacustrine sediments, ice cores, speleothems, peat deposits, corals, tree rings, and other natural archives preserve evidence of climatic fluctuations over seasonal to orbital timescales, providing the foundation for understanding Quaternary environmental evolution [1, 2]. These archives have preserved abrupt climate transitions, glacial–interglacial cycles, hydroclimatic variability, monsoon evolution, and ecosystem responses across a wide range of temporal and spatial scales [3]. Since each archive records only selected components of the climate system through distinct physical, chemical, or biological processes, modern palaeoclimate research increasingly relies on integrating multiple proxy records rather than interpreting individual archives in isolation. The development of large databases and synthesis products has transformed palaeoclimate research from individual site interpretation toward regional-to-global synthesis, proxy-model comparison, and climate field reconstruction [4–8].

Proxy records representing the same climatic event often show substantial differences in amplitude, transition duration, timing, spectral characteristics, and long-term variance. Such discrepancies are generally attributed to chronological uncertainty, regional climatic heterogeneity, seasonal sensitivity, ecological complexity, proxy calibration limitations, or analytical uncertainty [9, 10]. Although these factors contribute to inter-record variability, they do not fully explain apparent synchronous climatic events, often recorded with contrasting magnitudes or temporal structures. However, an increasing body of theoretical, observational, and proxy-system modelling studies suggests that many of these differences arise from the processes through which climate information is recorded, modified, preserved, and sampled within geological archives themselves [11–13]. Therefore, observed proxy records should not be regarded as direct measurements of past climate but rather as filtered representations whose characteristics depend on archive-specific response processes.

One of the principal controls governing climate-signal preservation is temporal integration, where environmental forcing is integrated over finite time windows during proxy formation and subsequent archive evolution. For stratigraphic archives, the effective temporal resolution of an observation depends on the mathematical convolution of environmental forcing with an archive-specific transfer function. The resulting attenuation of climatic variability depends on the combined influence of accumulation rate, sampling interval, post-depositional mixing, molecular diffusion, pore-water exchange, compaction, analytical averaging, and ecological response lags, each of which broadens the temporal bandwidth over which climate information is recorded [14–16]. Similar filtering mechanisms operate across a wide range of proxy systems, with their different physical origins. Ice-core isotope records are modified by firn diffusion [17], marine sediments are affected by bioturbation and sediment mixing [13, 18], speleothem proxies integrate hydrological residence times, and ecological proxies such as pollen or diatoms commonly show process-specific biological response lags and taphonomic filters. Therefore, two archives with comparable effective temporal integration may preserve climate variability in very similar ways despite different depositional environments. Records from the same archive type may show substantially different behaviour if their accumulation rates or post-depositional processes differ. This perspective changes the emphasis from archive identity to measurable physical processes controlling effective temporal resolution and climate-signal bandwidth.

The influence of temporal filtering has important implications for several active areas of Quaternary science. Reconstructions of abrupt climatic events including the Younger Dryas, Dansgaard–Oeschger oscillations, Heinrich stadials, and the 8.2 ka event, are generally compared using archives with different temporal bandwidths. High-resolution Greenland ice cores preserve these events as abrupt transitions occurring over years to decades [19–21]. Many marine sediment records preserve the same events as broader centennial-scale transitions due to lower sedimentation rates and post-depositional mixing [22, 23]. Comparisons between speleothem and lacustrine records of Holocene monsoon variability reveal contrasting expressions of the same climatic forcing, highlighting differences in archive response time rather than necessarily indicating contradictory climate histories [24]. These examples show that temporal resolution is not merely a technical characteristic of an archive but a first-order control on the climatic information ultimately preserved.

Over the past decade, major advances in Proxy System Models (PSMs) have substantially improved understanding of how climatic information is transformed into measurable proxy signals [11, 12]. Forward modelling frameworks including SedProxy and PRYSM explicitly simulate archive-specific recording processes such as bioturbation, sediment mixing, seasonality, and proxy calibration, improving quantitative interpretation of sedimentary and lacustrine records [13, 25]. More recent developments include measurement-error proxy system models, Bayesian forward-modelling frameworks, archive-specific calibration strategies, and uncertainty-aware proxy synthesis [26–29].

Parallel advances in paleoclimate data assimilation (PDA) and climate field reconstruction (CFR) have integrated proxy observations with climate model simulations to reconstruct past climate states, accounting for observational uncertainty via Ensemble Kalman Filtering and advanced data smoothers [30–34]. Proxy-system biases, coloured proxy noise, and archive-dependent uncertainties can substantially influence climate reconstructions and proxy-model comparisons [35–37]. These developments have significantly improved archive-specific interpretation and uncertainty quantification.

Despite these advances, most existing approaches remain archive-specific and require detailed parameterization of individual proxy systems. Therefore, they are not designed to provide a generalized quantitative framework for comparing climate-signal preservation across heterogeneous geological archives. A transferable screening framework based on common physical controls would complement existing Proxy System Models by providing first-order estimates of effective temporal resolution before detailed archive-specific modelling is undertaken.

This study develops a generalized quantitative framework for evaluating climate-signal preservation in Quaternary palaeoclimate archives based on common physical controls governing temporal integration. The framework introduces practical metadata-based estimates of effective temporal resolution together with generalized relationships describing amplitude attenuation and duration inflation across archives characterized by contrasting filtering mechanisms. Representative applications to Greenland ice cores, Chinese speleothems, and North Atlantic marine sediments show how readily available archive metadata can be translated into first-order estimates of climate-signal preservation. Rather than replacing archive-specific Proxy System Models, the proposed framework complements them by providing a transferable screening tool for comparing heterogeneous archives within a common temporal bandwidth.

2. Conceptual Framework and Methods

2.1. Framework Assumptions and Hypotheses

The proposed framework considers palaeoclimate archives as dynamic systems that transform climatic forcing into observable proxy signals. The objective is to identify the first-order controls driving climate-signal preservation, common across diverse Quaternary archives rather than to reproduce archive-specific physical or geochemical processes. Accordingly, the framework adopts four simplifying assumptions. (i) Climatic forcing is prescribed independently of the archive. (ii) Archive behaviour is approximated as a linear time-invariant system. (iii) Temporal filtering is represented by an effective response function. (iv) Chronological uncertainty and non-climatic noise are treated independently from physical filtering. These assumptions provide a generalized first-order description of climate-signal preservation that is consistent with the conceptual foundations of archive-specific Proxy System Models while remaining intentionally independent of any individual archive [11–13, 26]. The generalized sequence through which climate information is transformed from forcing to measured proxy signal is summarised schematically in Figure 1. Each stage may introduce temporal integration, filtering, attenuation, or non-climatic modification that influences the final observed record.

2.2. Climate Signals as Filtered Observations

The observed proxy record [$X_{\mathrm{obs}}(t)$] is represented as the convolution of the climatic forcing with the archive response function [$G(t)$].

$$X_{\mathrm{obs}}(t) = \int_{-\infty}^{\infty} X_{\mathrm{clim}}(\tau) G(t-\tau)\, d\tau + \varepsilon(t), \tag{1}$$

where $X_{\mathrm{clim}}(t)$ is the climatic forcing, $G(t)$ is the effective archive response function, and $\varepsilon(t)$ represents the combined effects of measured uncertainty, chronological uncertainty and non-climatic noise. Applying the Fourier transform produces $\widehat{X}_{\mathrm{obs}}(f)$.

$$\widehat{X}_{\mathrm{obs}}(f) = \widehat{X}_{\mathrm{clim}}(f)\widehat{G}(f) + \widehat{\varepsilon}(f). \tag{2}$$

The hats denote Fourier transforms and f denotes frequency. Equation (2) distinguishes climatic variability from archive-dependent attenuation and provides the basis for evaluating signal preservation in the frequency domain.

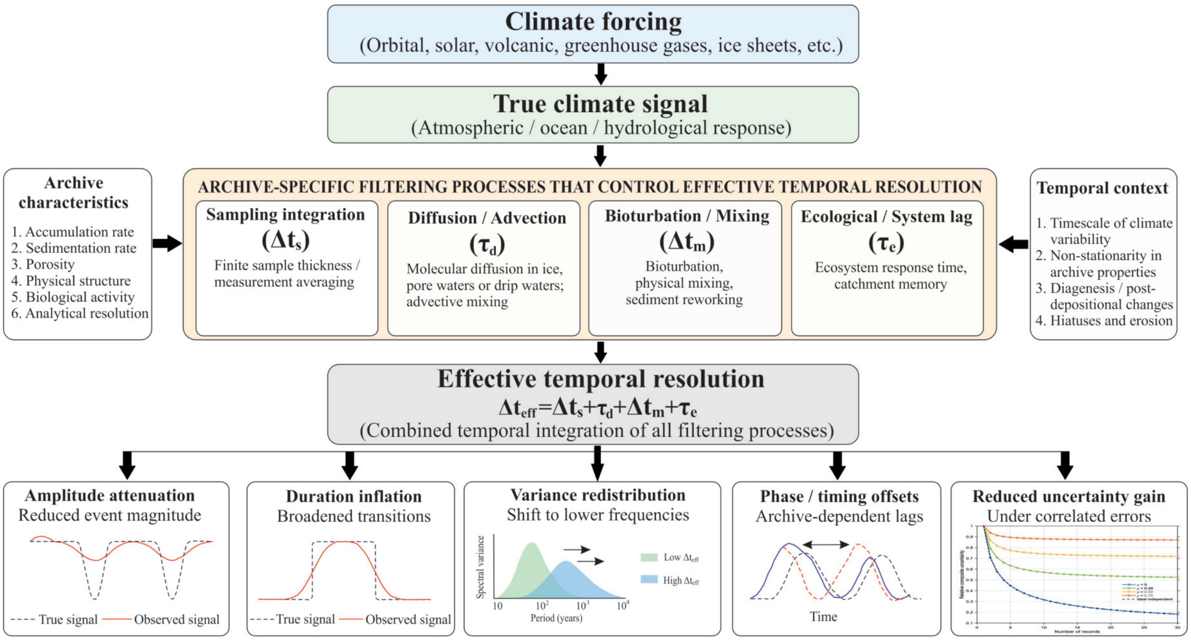

Figure 1. Generalized conceptual framework illustrating the transformation of climate signals from external forcing to observed palaeoclimate records. Coloured curves in the schematic panels represent the same climatic signal after progressively stronger temporal filtering (increasing Δt_{eff}).

2.3. Archive Transfer Function and Operational Bandwidth

The archive response is represented by the transfer function $\widehat{G}(f)$.

$$H(f) = \widehat{G}(f), \tag{3}$$

$H(f)$ represents the proportion of climatic variance transmitted at each frequency. The effective bandwidth of an archive is characterized by the cut-off frequency f_c, defined by the half-power criterion, corresponding to the conventional -3 dB point.

$$|H(f_c)|^2 = 0.5. \tag{4}$$

Frequencies exceeding f_c are progressively attenuated and contribute minimally to the observable proxy record. The transfer function provides a generalized description of frequency-dependent attenuation and forms the theoretical basis for interpreting the numerical experiments presented in Section 3.

2.4. Effective Temporal Resolution

The sampling-controlled temporal resolution is defined by Equation (5).

$$\Delta t_s = \frac{\Delta d}{R}, \tag{5}$$

where Δd is the sampling interval and R is the net accumulation rate. Additional temporal smoothing produced by sediment mixing or diffusion is represented as Δt_m.

$$\Delta t_m = \frac{L}{R}, \tag{6}$$

where L is the effective mixing depth. Assuming that individual smoothing processes contribute additively at first order, the effective temporal resolution is approximated by Δt_{eff}.

$$\Delta t_{\text{eff}} \approx \Delta t_s + \Delta t_m + \tau_d + \tau_e, \tag{7}$$

where Δt_s is the sampling-controlled temporal resolution, Δt_m is the characteristic temporal smoothing associated with sediment mixing or bioturbation, and τ_d and τ_e represent characteristic diffusion and ecological response times, respectively. Equation (7) is not intended as a mechanistic derivation but as a first-order operational approximation of the cumulative temporal smoothing imposed by the principal archive-filtering processes. The individual terms are combined linearly to provide a conservative heuristic estimate of the characteristic effective temporal resolution governing climate-signal preservation across diverse archive types. This simplified formulation is adopted to provide a transferable metric for inter-archive comparison rather than to describe the exact convolution of individual filtering processes, which may differ among proxy systems. Similar first-order effective timescale concepts have been used in proxy-system and forward-modelling studies to summarize the net influence of multiple smoothing processes [10–12]. Throughout this study, geological ages are expressed as ka BP (Before Present, referenced to 1950 CE), whereas yr and kyr denote durations or temporal intervals used in the numerical experiments and archive-response calculations.

2.5. Synthetic Climate Forcing

The synthetic forcing comprised four components: (i) a zero-trend baseline, (ii) orbital- to centennial-scale oscillations, (iii) abrupt climate transitions represented by Gaussian anomalies, and (iv) stochastic red noise following an AR(1) process. All realizations are generated at annual resolution over a 12 kyr interval using a fixed computational time step ($\Delta t = 1$ yr) with fixed boundary conditions to ensure numerical reproducibility. Parameter values are summarized in Table 1. Synthetic climate forcing is defined by Equation (8).

$$X_{\text{clim}}(t) = T(t) + \sum_{i=1}^{n} A_i \sin(2\pi f_i t + \phi_i) + \sum_{j=1}^{m} E_j(t) + N(t) \tag{8}$$

$T(t)$ is the long-term climatic trend, A_i, f_i and ϕ_i describe oscillatory components, $E_j(t)$ represents abrupt climatic events, and $N(t)$ is stochastic noise. Synthetic forcing is generated using a fixed computational time step ($\Delta t = 1$ yr) and convolved with Gaussian response kernels characterized by standard deviations (σ_{G}) ranging from 10 to 1000 yr. The Gaussian kernel width controls the degree of numerical smoothing applied during the forward experiments. A series of numerical experiments is carried out by varying the Gaussian kernel width (σ_{G}) and sampling interval (Δt_{s}) while maintaining identical climatic forcing to isolate the influence of temporal integration on climate-signal preservation. The synthetic forcing provides a controlled benchmark for evaluating the influence of temporal integration independently of archive-specific proxy-system processes. In the synthetic forward experiments, the Gaussian response kernel is parameterized by its standard deviation (σ_{G}). For the purposes of these numerical experiments, the study adopts the operational definition $\Delta t_{\text{eff}} = \sigma_{\text{G}}$. This equivalence is a study-specific numerical convention introduced solely to provide a common measure of temporal smoothing and should not be interpreted as a universally applicable physical relationship. For a Gaussian response kernel, the corresponding full width at half maximum (FWHM) is given by FWHM = $2.355\sigma_{\text{G}}$. In contrast, for natural archives, Δt_{eff} is estimated independently from measurable archive properties using Equation (7). Therefore, the numerical experiments and the practical archive applications employ the same operational descriptor (Δt_{eff}), although obtained by different methods.

2.6. Chronological Uncertainty Propagation

Chronological uncertainty is represented using Gaussian age perturbations to illustrate the influence of age uncertainty on reconstructed climate signals independently of physical archive filtering. The observed chronology is represented as $t^{(k)}$.

$$t^{(k)} = t_{\text{true}} + \delta_t^{(k)} \tag{9}$$

$\delta_t^{(k)}$ denotes the kth realization sampled from the age-depth covariance matrix, $\delta_t^{(k)} \sim \mathcal{N}(0, \Sigma_{\text{age}})$.

The filtered archive state for each realization is defined as $X_{\text{obs}}^{(k)}$.

$$X_{\text{obs}}^{(k)} = \int X_{\text{clim}} G(t^{(k)} - \tau) d\tau + \varepsilon(t). \tag{10}$$

An ensemble of 1000 realizations was adopted to generate uncertainty envelopes for the filtered climate signals. Ensemble means together with 95% confidence intervals ($\pm 2\sigma$) were used to summarize chronological uncertainty.

2.7. Quantitative Performance Metrics

Framework performance is evaluated using two dimensionless indices; amplitude retention (R_A) and Duration inflation (D_I).

$$R_A = \frac{A_{\text{obs}}}{A_{\text{clim}}}, \tag{11}$$

$$D_I = \frac{D_{\text{obs}}}{D_{\text{clim}}}. \tag{12}$$

2.8. Numerical Experiments

Numerical experiments are conducted by convolving the prescribed synthetic climatic forcing with Gaussian response kernels having progressively increasing standard deviations ($\sigma_{\text{G}} = 10$–1000 yr). Increasing σ_{G} represents progressively stronger temporal smoothing and, within the synthetic forward experiments, is interpreted as the corresponding effective temporal resolution (Δt_{eff}). This study-specific convention enables direct comparison between the numerical experiments and the metadata-based estimates of Δt_{eff} derived for representative Quaternary archives using Equation (7), without affecting the numerical calculations or their interpretation. The response width is systematically varied to represent archives spanning annual to millennial effective temporal resolutions. Model behaviour is evaluated in terms of attenuation of climatic-event amplitude, inflation of apparent event duration, redistribution of spectral variance, and the influence of temporal filtering on the preservation of climate signals. All simulations are performed using identical climatic forcing so that differences among simulated records arose solely from archive response characteristics. Convolution is performed using the normalized Gaussian response kernel while retaining the original time-series length throughout the numerical experiments. To minimize boundary effects associated with convolution, only the central portion of the filtered time series is interpreted when evaluating event amplitude and duration.

2.9. Practical Application

The practical applicability of the proposed framework is evaluated using representative Quaternary archives that encompass the principal mechanisms of temporal filtering: the North Greenland Ice Core Project (NGRIP) ice core, a Chinese speleothem record, and ODP Site 980 marine sediments. Published archive characteristics, including sampling interval, accumulation rate, diffusion length, and mixed-layer depth, are used to estimate effective temporal resolution (Δt_{eff}) for each archive. The generalized relationships developed in this study are used to estimate the expected attenuation of climatic-event amplitude and inflation of apparent event duration. These representative applications are intended to illustrate how readily available archive metadata can be translated into first-order predictions of climate-signal preservation rather than to replace archive-specific proxy-system models.

Table 1. Parameters used to generate the synthetic climate forcing used in the numerical forward experiments. The parameter values are selected to represent characteristic temporal scales commonly encountered in Quaternary palaeoclimate records rather than any specific archive or geographical region. The synthetic forcing is intended to provide a generalized benchmark for evaluating archive response, temporal filtering, and uncertainty propagation under controlled conditions. Parameter ranges are chosen to encompass the effective temporal resolutions of annually resolved archives (e.g., ice cores and tree rings) through low-resolution marine and lacustrine sediment records.

Parameter	Symbol	Mathematical Definition/Value	Units	Purpose/Geological Justification
Simulation duration	T	12,000	yr	Covers the Late Glacial–Holocene transition, including the Younger Dryas and Holocene climatic evolution.
Computational time step	Δt	1	yr	Fixed numerical integration time step used to generate the synthetic climate forcing and perform forward simulations. It is independent of archive temporal resolution.
Long-term climatic trend	$T(t)$	0	–	Zero baseline adopted to isolate archive filtering effects from secular climatic trends.
Orbital-frequency component	f_1	1/10,000	yr^{-1}	Represents long-period orbital-scale variability.
Millennial-frequency component	f_2	1/1000	yr^{-1}	Represents sub-orbital variability such as Bond-type or millennial climate oscillations.
Centennial-frequency component	f_3	1/200	yr^{-1}	Represents high-frequency Holocene climate variability.
Oscillation amplitudes	A_i	1.0 (normalized)	Dimensionless	Equal amplitudes adopted to isolate frequency-dependent attenuation.
Phase angles	ϕ_i	Random (0–2π)	rad	Prevents artificial phase alignment among sinusoidal components.
Abrupt event function	$E(t)$	Gaussian anomaly	–	Represents rapid climate transitions comparable to the Younger Dryas or 8.2 ka event.
Abrupt event magnitude	A_e	$-2.5\ \sigma$	Dimensionless	Represents a pronounced climatic excursion relative to background variability.
Abrupt event duration	σ_e	100	yr	Characteristic duration of abrupt climate transitions.
Background noise model	$N(t)$	AR(1) process	–	Represents persistent climatic variability.
Noise standard deviation	σ_N	5% of total signal variance	%	Represents moderate proxy and environmental noise while maintaining signal detectability.
Gaussian kernel width	σ_{G}	10–1000	yr	Standard deviation of the Gaussian response kernel used to simulate archive-dependent temporal smoothing. Larger values represent progressively stronger smoothing.
Sampling interval	Δt_s	1–200	yr	Temporal interval between successive archive observations used to define the sampling component of temporal resolution.
Effective temporal resolution*	Δt_{eff}	Derived using Equation (7)	yr	First-order operational estimate of the cumulative temporal smoothing imposed by sampling integration, mixing, diffusion, and ecological response. Used for interpretation rather than as a direct numerical input.

* The computational time step (Δt), sampling interval (Δt_s), Gaussian kernel width (σ_{G}), and effective temporal resolution (Δt_{eff}) represent distinct quantities. Δt defines the numerical discretization of the simulations, Δt_{s} characterizes the temporal spacing of archive observations. Within the synthetic forward experiments only, Δt_{eff} is operationally taken to be equal to σ_{G}; this convention is adopted for numerical implementation and does not imply a general physical equivalence for natural archives.

3. Results

3.1. Impact of Temporal Smoothing

Forward modelling shows that increasing effective temporal smoothing ($\Delta t_{\rm eff}$) systematically changes the observable structure of climate signals. When smoothing is weak (10–30 yr), the filtered series closely resembles the original signal, retaining much of the short-period variability and preserving the abrupt event near the centre of the record (Figure 2). As $\Delta t_{\rm eff}$ increases into the centennial range and beyond, higher-frequency fluctuations are progressively damped, and the signal becomes increasingly dominated by lower-frequency structure.

At the strongest smoothing levels (300–700 yr), the record cannot resolve decadal to multi-decadal variability. Instead, the filtered signal is dominated by broad centennial- to millennial-scale fluctuations. Although the abrupt negative excursion remains identifiable, its peak amplitude is reduced and its boundaries become progressively less distinct. These simulations show that increasing effective temporal smoothing systematically suppresses short-period variability while preserving broader climatic structure.

3.2. Decline in Event Amplitude

The magnitude of transient events decreases monotonically with increasing $\Delta t_{\rm eff}$ (Figure 3). Relative peak amplitude is highest under weak decadal smoothing and declines rapidly as the effective averaging window enters the centennial range. Beyond this threshold, additional smoothing continues to reduce peak magnitude, although at a slower rate.

These results show that increasing effective temporal smoothing produces predictable attenuation of transient climatic events, with the greatest reduction occurring as $\Delta t_{\rm eff}$ increases from decadal to centennial timescales.

3.3. Smoothing Inflates Apparent Event Duration

Numerical experiments show that increasing $\Delta t_{\rm eff}$ broadens the apparent duration of abrupt climate events (Figure 4A). With increasing smoothing, transitions become more gradual, and the duration of threshold exceedance is substantially prolonged.

Comparison of the numerical simulations with the analytical broadening model (Figure 4B) shows close agreement across the investigated range of effective temporal smoothing. Both approaches show that apparent event duration increases systematically with increasing $\Delta t_{\rm eff}$, indicating that duration inflation follows a predictable relationship with temporal integration.

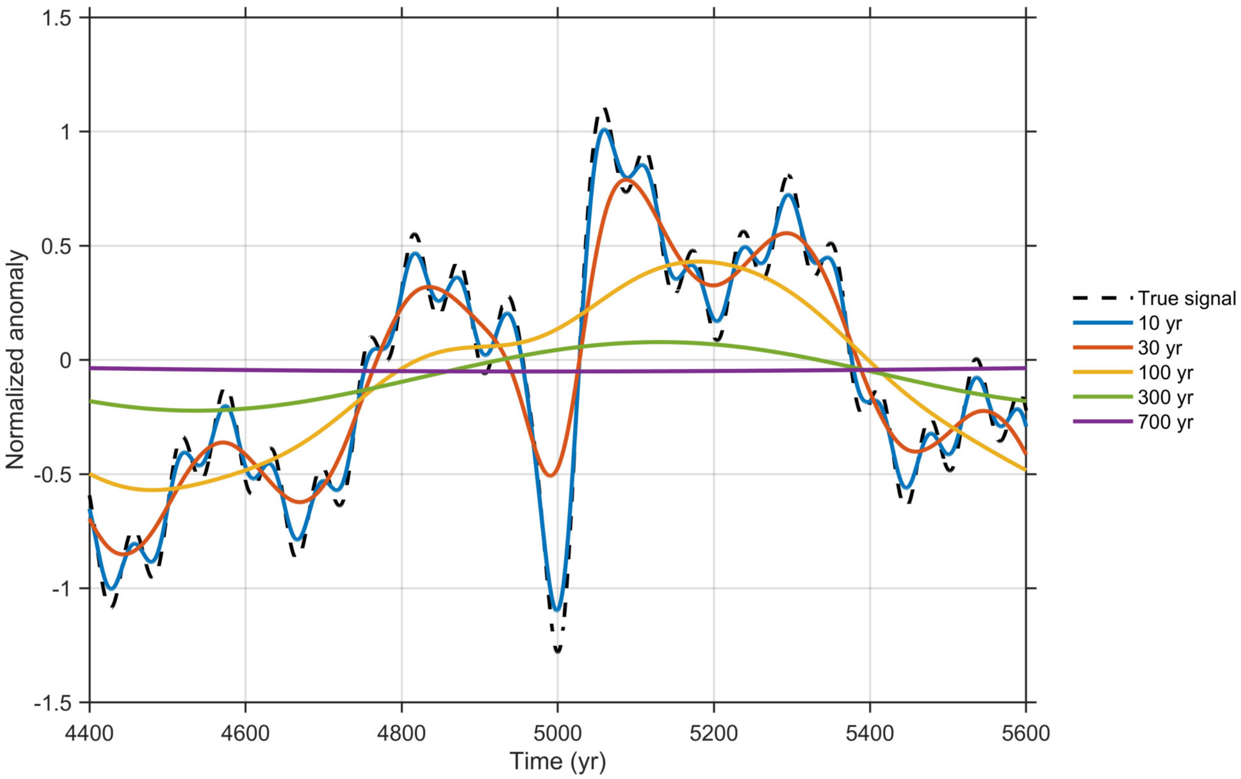

Figure 2. Forward-modelled response of a synthetic climate signal to increasing effective temporal smoothing $(\Delta t_{\rm eff})$. Weak smoothing preserves short-period variability and the sharp expression of the abrupt event. Stronger smoothing progressively suppresses high-frequency fluctuations, reduces peak magnitude, and enhances the relative prominence of longer-timescale structure.

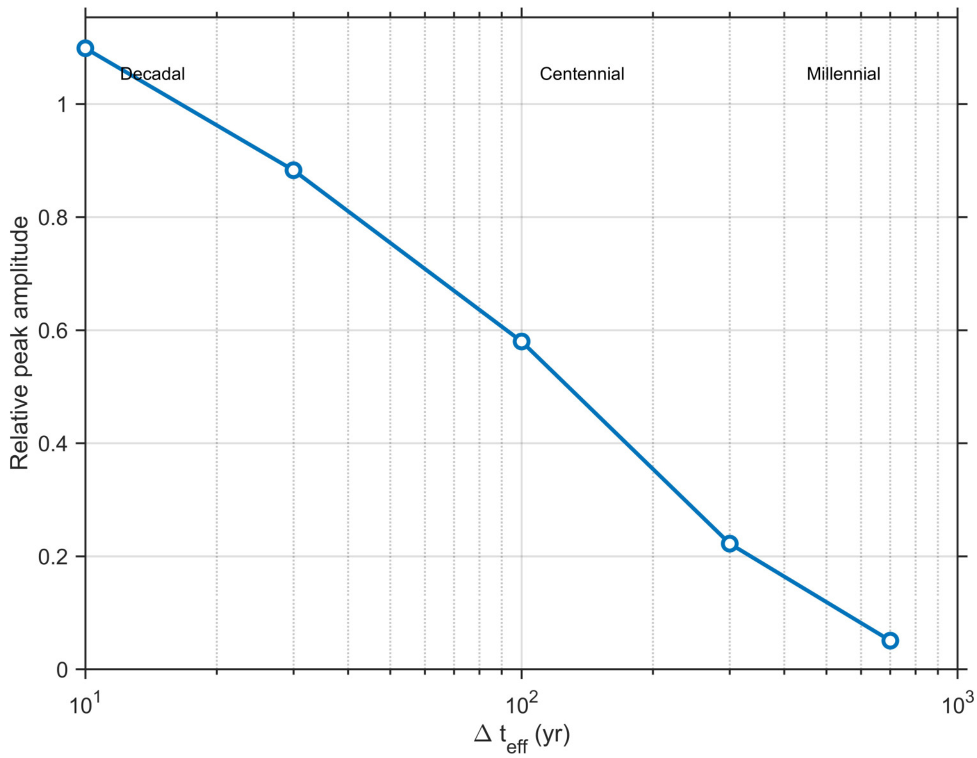

Figure 3. Decline in relative peak amplitude with increasing effective temporal smoothing (Δt_{eff}). Short-lived climate events are progressively attenuated as the averaging window increases from decadal to centennial and millennial scales.

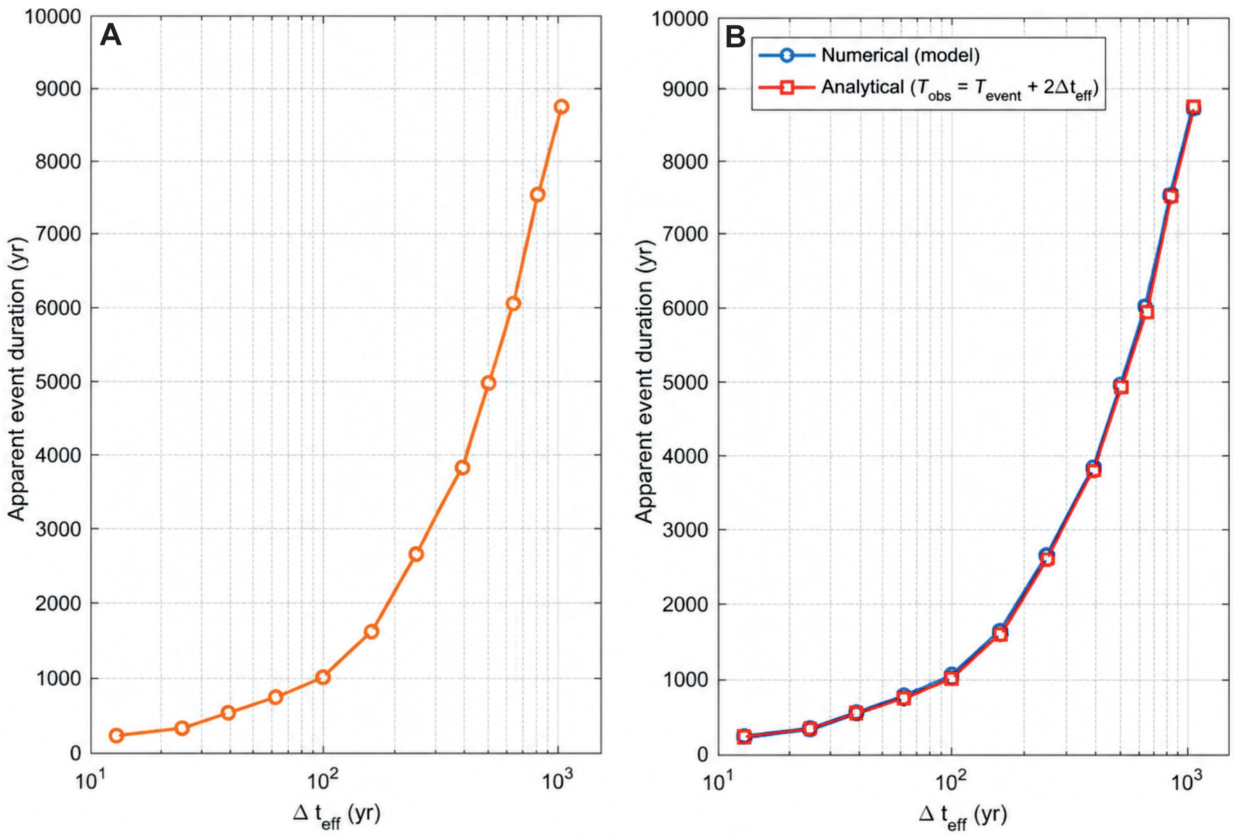

Figure 4. Broadening of abrupt climate events with temporal smoothing. (**A**) Simulated increase in apparent event duration with increasing effective temporal resolution (Δt_{eff}). (**B**) Numerical forward-model results compared with the first-order analytical broadening relationship represented by Equation (7), showing close agreement over the investigated range of temporal smoothing.

3.4. Variance Redistribution

Spectral analysis shows a systematic redistribution of variance across frequency bands with increasing effective temporal smoothing (Δt_{eff}) (Figure 5). Under weak smoothing (10–30 yr), a substantial proportion of the total variance is concentrated at periods shorter than 100 years. As Δt_{eff} increases into the centennial and millennial range, short-period variance decreases progressively, whereas the relative contribution of centennial (100–1000 yr) and millennial ($>$1000 yr) variability increases.

At the highest smoothing levels, low-frequency variability dominates the filtered signal. This increase is relative rather than absolute because higher-frequency variance is preferentially removed during temporal filtering. Therefore, the remaining variance is increasingly concentrated within longer-period components of the signal.

3.5. Effect of Correlated Errors

Theoretical stacking experiments show that composite uncertainty decreases with increasing numbers of records, although the rate of reduction depends strongly on the correlation structure of the underlying errors (Figure 6). When errors are independent ($\rho = 0$), uncertainty decreases approximately according to the inverse square-root relationship expected from statistical averaging.

As inter-record error correlation increases, uncertainty reduction becomes progressively weaker. For strongly correlated cases ($\rho = 0.75$), additional records provide only modest reductions in uncertainty, and composite uncertainty approaches an asymptotic limit.

3.6. Contrasting Archive Responses to an Abrupt Climate Event

A conceptual abrupt climate event illustrates how identical climatic perturbations may be expressed differently in archives possessing contrasting effective temporal resolutions (Figure 7). The high-resolution archive closely preserves the abrupt onset and termination of the imposed event, whereas the low-resolution archive records a broader, attenuated anomaly with more gradual transitions.

The numerical experiment shows that increasing temporal integration alone modifies the observed duration, amplitude, and transition gradient of an identical climatic event. The differences arise solely from variations in effective temporal smoothing while the underlying forcing remains unchanged. Increasing effective temporal smoothing systematically attenuates peak amplitude, broadens apparent event duration, redistributes variance toward longer-period variability, and limits uncertainty reduction under correlated errors. These behaviours are reproduced consistently across the forward simulations and provide the quantitative basis for the practical applications presented in the following section.

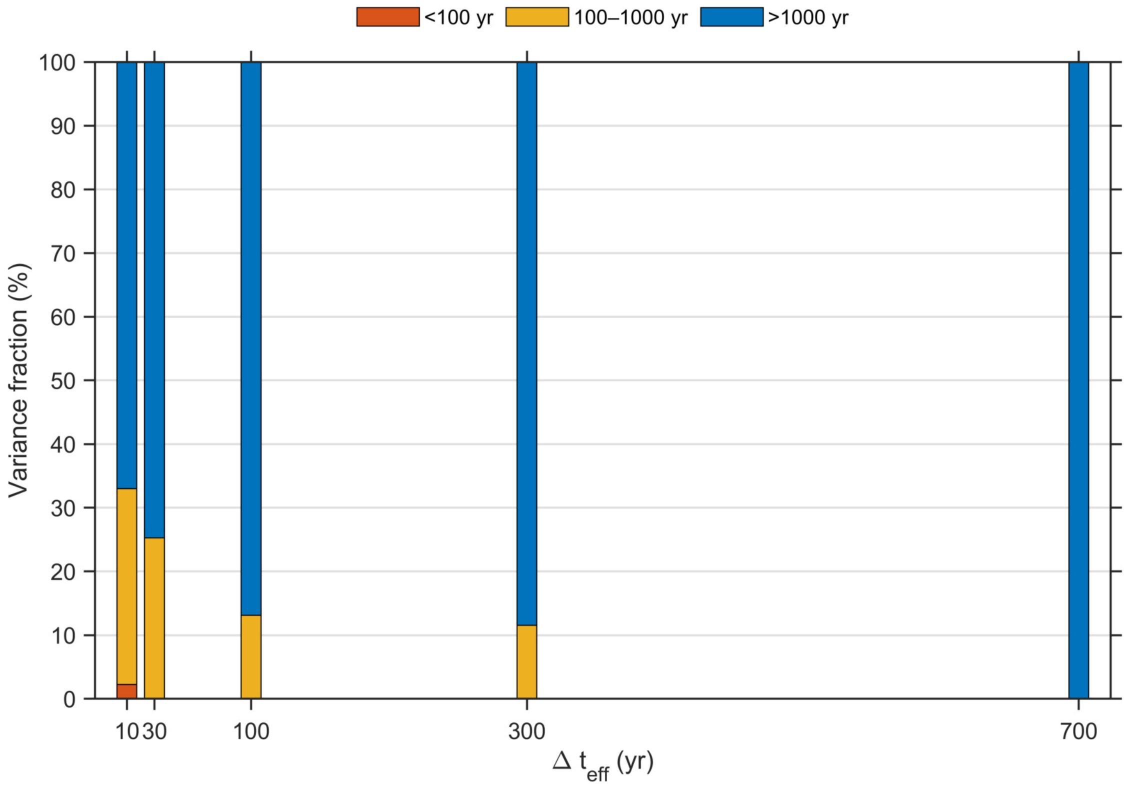

Figure 5. Redistribution of variance fraction across frequency bands under increasing effective temporal smoothing (Δt_{eff}). Progressive filtering suppresses variability at periods shorter than 100 years and increases the relative contribution of centennial (100–1000 yr) and millennial ($>$1000 yr) variability.

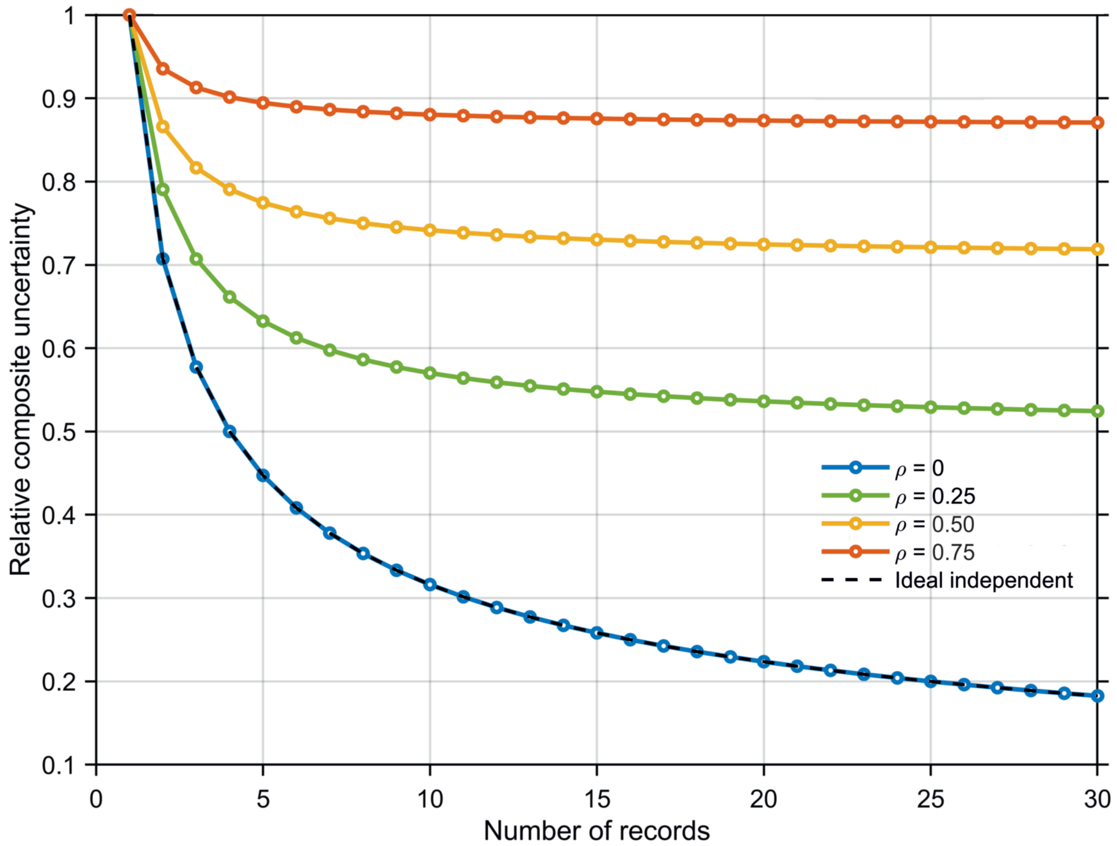

Figure 6. Effect of correlated uncertainties on uncertainty reduction through multi-record averaging. Independent errors ($\rho = 0$) follow the inverse square-root expectation, whereas increasing inter-record correlation limits the decrease in composite uncertainty and produces an asymptotic floor.

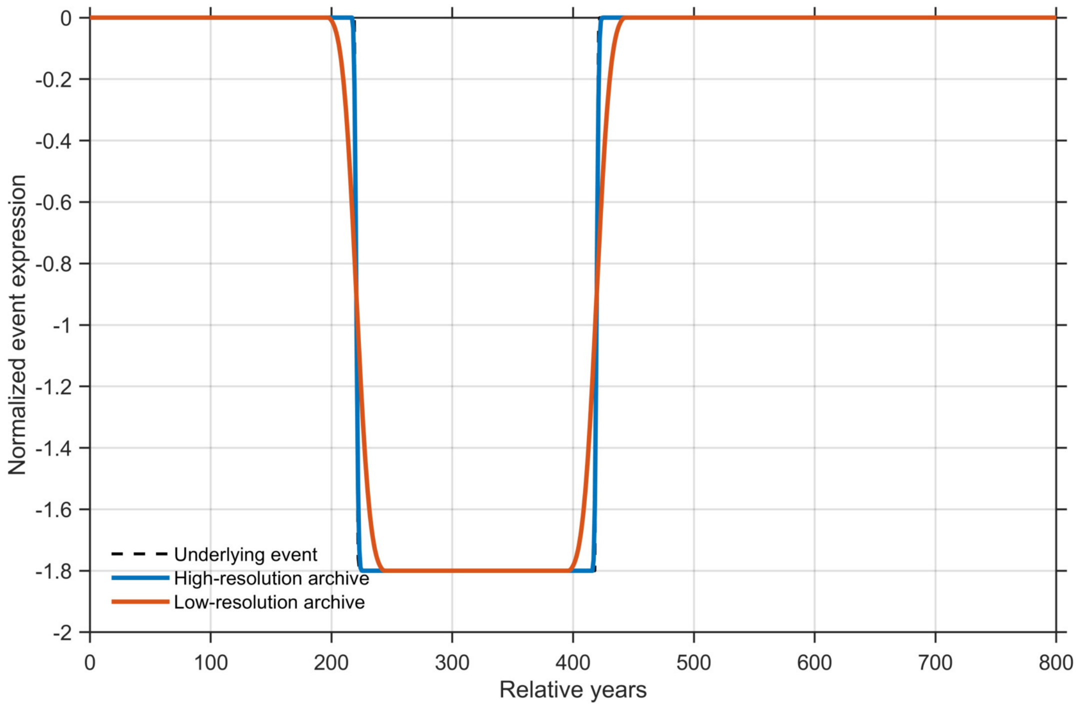

Figure 7. Conceptual illustration of contrasting archive expressions of the same abrupt climate event. A high-resolution archive preserves relatively sharp onset and termination, whereas a lower-resolution archive records a broader and attenuated anomaly because of stronger temporal integration.

4. Practical Application of the Generalized Temporal-Filtering Framework

To evaluate the practical application of the proposed framework, it is applied to three representative Quaternary archives that encompass the principal mechanisms of temporal filtering encountered in palaeoclimate research: diffusion-dominated Greenland ice cores, sampling-dominated Chinese speleothems, and bioturbation-dominated North Atlantic marine sediments. These archives are selected because together they span nearly two orders of magnitude in effective temporal resolution and represent the dominant classes of archive-dependent climate-signal filtering. The objective of these worked examples is not to reproduce individual proxy records or replace archive-specific Proxy System Models, but to examine how readily available archive metadata can be translated into first-order estimates of effective temporal resolution (Δt_{eff}), climate-signal attenuation, and duration inflation using the generalized framework developed in this study. All parameter values are derived from published archive characteristics, allowing the workflow to be readily transferred to other Quaternary records.

Increasing effective temporal resolution systematically alters the preservation of climatic events by reducing their observed amplitudes and progressively broadening their apparent durations (Figure 8). These generalized relationships allow readily available archive metadata to be translated directly into first-order predictions of climate-signal attenuation and duration inflation across diverse Quaternary archives. Rather than replacing archive-specific Proxy System Models, the framework provides a practical screening tool for evaluating archive comparability based on common temporal-filtering processes.

Increasing effective temporal resolution also systematically redistributes the preserved climatic variance across different frequency bands (Figure 9). Under weak temporal filtering, most of the preserved variance remains concentrated at periods shorter than 100 years, indicating that high-frequency climatic variability is retained with little attenuation. As effective temporal resolution increases into the centennial range, the contribution of short-period variability decreases progressively, whereas centennial-scale variability becomes increasingly dominant. Under the strongest temporal filtering, high-frequency variability is largely removed and the preserved signal becomes dominated by millennial-scale climatic variability.

These systematic changes explain the contrasting spectral characteristics of representative Quaternary archives (Figure 9). NGRIP retains most climatic variance at periods shorter than 100 years because its effective temporal resolution remains only a few years. Chinese speleothems occupy an intermediate position where centennial-scale variability becomes increasingly important while much of the short-period variability is attenuated. ODP Site 980 preserves predominantly millennial-scale variability because prolonged temporal integration suppresses higher-frequency climate fluctuations. These representative applications show that differences among archives arise not only from depositional environment but also from the temporal bandwidth over which climatic information is preserved. Therefore, two archives responding to identical climatic forcing may preserve very different portions of the climatic spectrum solely because of differences in effective temporal resolution.

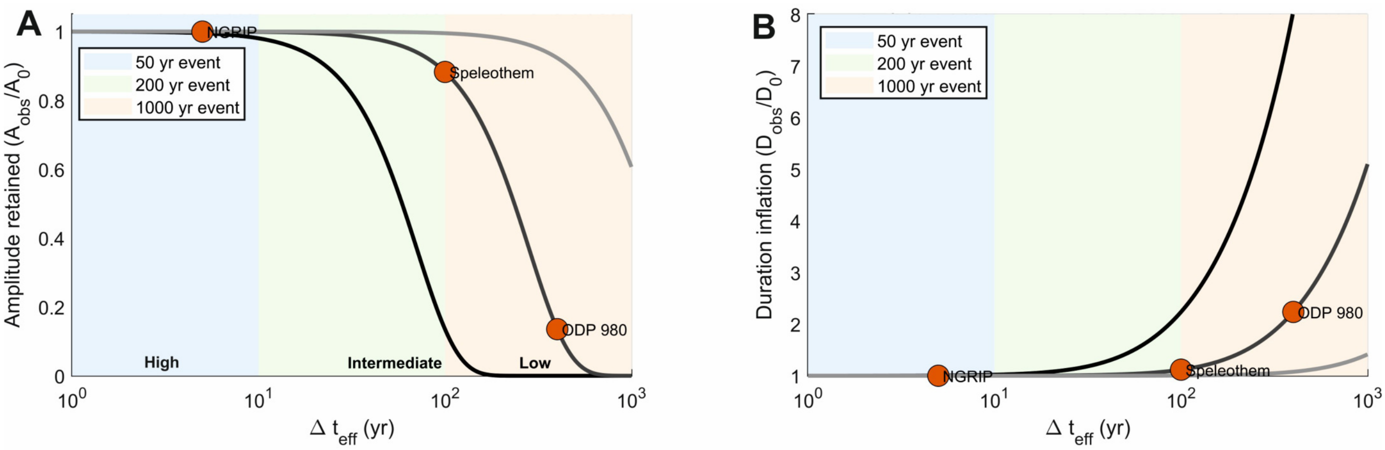

Figure 8. Practical framework for estimating archive-dependent climate-signal filtering. (**A**) Amplitude attenuation as a function of effective temporal resolution (Δt_{eff}) for reference climate events of 50, 200 and 1000 years duration. (**B**) Inflation of apparent event duration with increasing Δt_{eff} for the same event lengths. Symbols indicate representative worked examples from the NGRIP ice core, a Chinese speleothem record, and ODP Site 980 marine sediments.

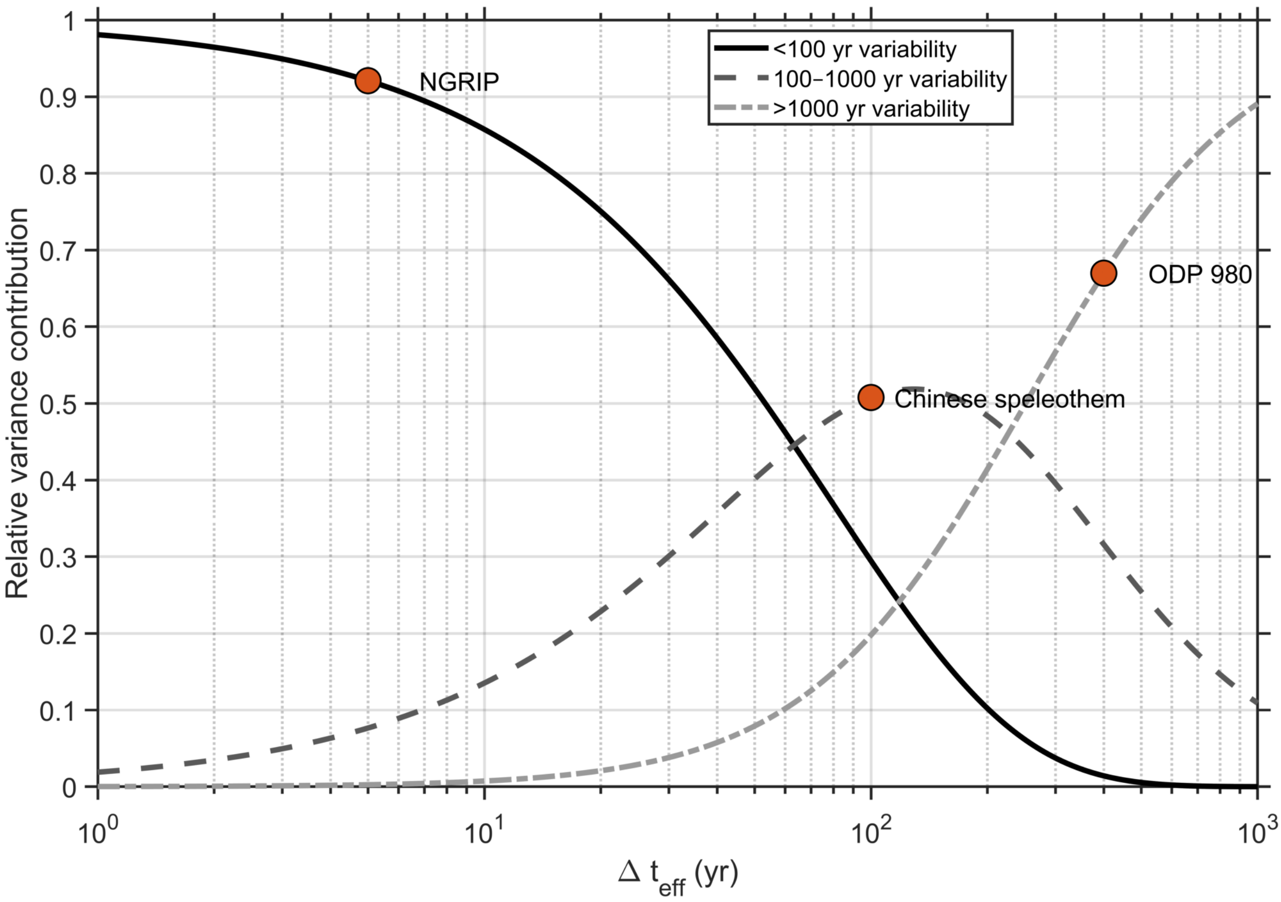

Figure 9. Representative application of the generalized temporal-filtering framework to Quaternary palaeoclimate archives. Curves illustrate the predicted redistribution of spectral variance with increasing effective temporal resolution (Δt_{eff}). Orange symbols denote representative archive positions based on published estimates of effective temporal resolution for the North Greenland Ice Core Project (NGRIP), Chinese speleothems, and ODP Site 980 marine sediments. Increasing Δt_{eff} progressively suppresses high-frequency ($<$100 yr) variability while enhancing the relative contribution of centennial (100–1000 yr) and millennial ($>$1000 yr) climate variability.

4.1. NGRIP Greenland Ice Core: Diffusion-Controlled Filtering

The North Greenland Ice Core Project (NGRIP) provides a representative example of a diffusion-dominated archive in which effective temporal resolution is controlled primarily by annual accumulation and firn diffusion. Annual layer thicknesses in deep NGRIP ice are approximately 1.1 cm yr^{-1}, while isotopic diffusion lengths reported for comparable Greenland ice range from approximately 3.5 to 6 cm depending on ice properties and impurity content [14, 19]. Using a representative sampling interval of 1 cm, the sampling component of temporal resolution is approximately 0.9 years.

$$\Delta t_s = \frac{\Delta d}{\lambda} = \frac{1}{1.1} \approx 0.9 \text{ yr}.$$

Diffusive smoothing contributes an additional effective timescale of approximately 3–5 years.

$$\tau_d = \frac{\sigma}{\lambda} \approx 3.2\text{–}5.5 \text{ yr}.$$

Such values place NGRIP within the high-resolution region of the generalized attenuation and duration-inflation relationships (Figure 8). Because effective temporal integration remains minimal, climatic events lasting several decades to centuries retain almost their full original amplitudes while experiencing negligible duration inflation. The corresponding position in Figure 9 indicates that most preserved climatic variance remains concentrated at periods shorter than 100 years, explaining Greenland ice cores' record of abrupt climatic transitions and high-frequency climate variability.

4.2. Chinese Speleothem Record: Sampling-controlled Filtering

The Chinese speleothem record of Cheng et al. [24] represents a sampling-dominated archive in which temporal resolution is governed primarily by growth rate and analytical sampling because post-depositional diffusion is negligible after calcite precipitation. It provides a useful example because its chronology and sampling strategy are exceptionally well constrained. The published temporal resolution varies between approximately 70 and 200 years, with average values of about 85–120 years. In the absence of significant post-depositional smoothing, the effective temporal resolution can be approximated by the sampling resolution itself.

$$\Delta t_{\text{eff}} \approx 85\text{–}120 \text{ yr.}$$

These values place the archive within the intermediate temporal-filtering regime (Figure 8), where centennial-scale climatic events experience only modest attenuation whereas shorter climatic fluctuations become progressively smoothed. Duration inflation remains modest, allowing major Holocene climatic transitions to retain their overall temporal structure despite partial suppression of higher-frequency variability. As illustrated in Figure 9, the preserved climatic variance shifts progressively from periods shorter than 100 years towards centennial variability, explaining the smoother appearance of speleothem records relative to annually resolved ice-core archives.

4.3. ODP Site 980: Bioturbation-Controlled Filtering

Marine sediments provide a contrasting example because temporal resolution is commonly limited not only by sampling strategy but also by biological mixing within the sediment column. ODP Site 980, a widely used North Atlantic palaeoclimate archive, shows an average sedimentation rate of approximately 15.2 cm kyr^{-1} over the interval considered here [38]. For a representative sampling interval of 1 cm, the sampling component of temporal resolution is approximately 66 years.

$$\Delta t_s = \frac{1}{15.2} \times 1000 \approx 66 \text{ yr.}$$

However, bioturbation typically mixes several centimetres of sediment in North Atlantic hemipelagic environments. Assuming a representative mixed-layer depth of 5 cm [13, 39], the bioturbation-induced smoothing timescale becomes approximately 329 years. The assumed mixed-layer depth is illustrative rather than site-specific; users can substitute locally constrained values where available.

$$\Delta t_m = \frac{5}{15.2} \times 1000 \approx 329 \text{ yr.}$$

Therefore, the combined effective temporal resolution is approximately 400 years.

$$\Delta t_{\text{eff}} \approx 395 \approx 400 \text{ yr.}$$

Such large effective temporal resolution places ODP Site 980 within the strongly filtered region of the generalized attenuation and duration-inflation relationships (Figure 8, Table 2), where abrupt climatic events are substantially attenuated and their apparent durations become markedly inflated. Under these conditions, only a small proportion of the original amplitude of a representative 200-year climatic event is retained. The corresponding position in Figure 9 shows that most preserved climatic variance occurs at millennial rather than centennial or decadal timescales, demonstrating how sediment mixing and bioturbation preferentially preserve long-period climate variability while suppressing shorter climatic fluctuations. Representative calculations for the three worked examples are summarized in Table 2.

Although the numerical values presented here are representative rather than site-specific, the workflow is directly transferable to any Quaternary archive for which sampling interval, accumulation rate, and principal smoothing mechanisms are known. Users may substitute site-specific parameters to obtain archive-specific estimates of effective temporal resolution and expected climate-signal preservation.

4.4. Implications for Archive Comparison

The representative applications show that increasing effective temporal resolution systematically modifies both the amplitude and spectral characteristics of preserved climate signals. High-resolution archives such as Greenland ice cores retain most short-period climatic variability with minimal attenuation or duration inflation, whereas intermediate-resolution speleothems preferentially preserve centennial-scale variability. Low-resolution marine sediments largely retain only millennial-scale climatic variability because stronger temporal integration suppresses shorter-period fluctuations. Together, Figures 8 and 9 show that readily available archive metadata can be translated into quantitative first-order estimates of climate-signal attenuation, duration inflation, and preserved climatic bandwidth, thereby providing a practical basis for evaluating whether different Quaternary archives can be meaningfully compared at a given temporal scale.

Table 2. Application of the generalized temporal-filtering framework to representative Quaternary archive types. Effective temporal resolution (Δt_{eff}) is estimated from published archive characteristics, and the corresponding amplitude retention and duration inflation are obtained from the generalized lookup relationships developed in this study for a representative 200-year climatic event.

Archive	Dominant Filtering Process	Estimated Δt_{eff} (yr)	Amplitude Retained (%)	Duration Inflation ($\times$)
NGRIP ice core	Diffusion	5	~100	1.00
Chinese speleothem	Sampling integration	100	~88	1.12
ODP Site 980 marine sediment	Bioturbation + sampling	400	~14	2.24

5. Discussion

5.1. Physical Controls on Climate-signal Preservation

The principal outcome of this study is that climate-signal preservation in Quaternary archives is governed primarily by measurable physical processes controlling temporal integration rather than by archive type alone. Conventional classifications such as marine sediments, ice cores, speleothems, peat deposits, and lacustrine records provide useful geological descriptions, but they do not uniquely determine temporal resolution or climatic fidelity. Even archives belonging to the same category may preserve climate variability very differently because of variations in accumulation rate, sampling interval, diffusion, sediment mixing, ecological response time, or post-depositional alteration. Archives formed within entirely different depositional environments may show comparable signal preservation when their effective temporal resolutions are similar.

The numerical experiments and representative applications presented in this study show that effective temporal resolution provides a common quantitative descriptor linking these diverse archive-specific processes. Rather than treating archive identity as a proxy for data quality or climatic fidelity, the framework emphasizes measurable physical controls that determine the temporal bandwidth over which climatic information is preserved. This generalized relationship between effective temporal resolution and preserved climatic bandwidth is summarized conceptually in Figure 10. This perspective provides a transferable basis for comparing heterogeneous Quaternary records and for identifying the timescales over which climatic variability can be reconstructed with confidence.

Tree rings and Greenland ice cores occupy the highest-fidelity end of the conceptual spectrum because rapid accumulation and minimal post-depositional modification preserve much of the original climatic variability. Speleothems occupy an intermediate position owing to hydrological integration and analytical sampling, whereas lacustrine and marine sediments preferentially retain longer-timescale variability because sediment mixing and lower accumulation rates progressively suppress higher-frequency climate signals.

The practical applications presented in Section 4 show that effective temporal resolution can be estimated directly from readily available archive metadata. Therefore, first-order predictions of amplitude attenuation and duration inflation can be obtained without detailed archive-specific modelling. Although simplified, this approach provides an operational framework for evaluating the temporal comparability of palaeoclimate archives prior to more detailed proxy-system investigations.

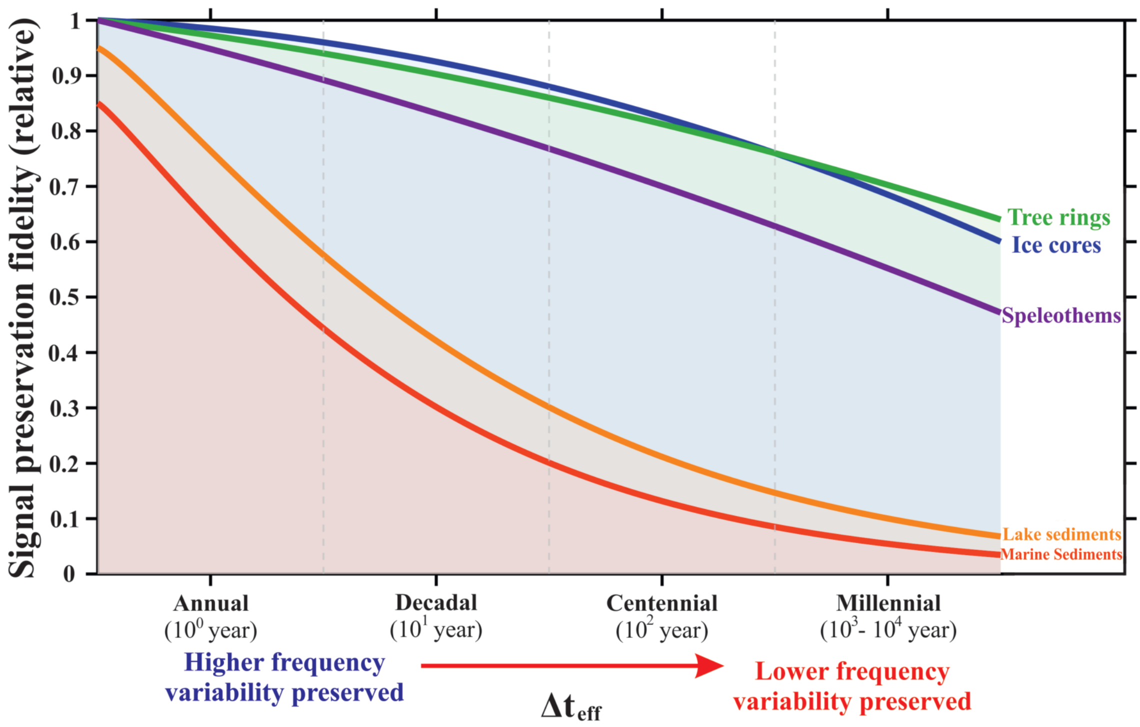

Figure 10. Conceptual comparison of temporal bandwidth preservation in major Quaternary palaeoclimate archives. High-resolution archives such as ice cores and tree rings efficiently preserve high-frequency variability. Lacustrine and marine archives capture lower-frequency climatic variability efficiently due to stronger temporal integration and post-depositional smoothing.

5.2. Implications for Abrupt Climate Events

One of the clearest consequences of archive-dependent temporal filtering is its influence on the apparent expression of abrupt climatic events (Figure 7). The representative applications developed in Section 4 show that differences in effective temporal resolution alone can substantially modify the observed amplitude and duration of climatic transitions despite identical underlying forcing. Therefore, abrupt climate events preserved in different archives cannot necessarily be compared directly without considering the temporal integration characteristics of each archive. This principle has important implications for the interpretation of major Quaternary climate events, including the Younger Dryas, Dansgaard–Oeschger oscillations, Heinrich stadials, and the 8.2 ka event. Greenland ice-core records preserve many of these events with annual-to-decadal resolution because diffusion lengths remain small relative to accumulation rates, whereas marine sediment records frequently integrate the same climatic transitions over centuries because of lower sedimentation rates, sampling integration, and bioturbation. The contrasting expressions observed among these archives need not imply contradictory climate histories but may instead reflect predictable differences in archive response.

This interpretation does not suggest that temporal filtering is the sole explanation for discrepancies among palaeoclimate records. Regional climatic heterogeneity, proxy-specific sensitivity, ecological response, and chronological uncertainty remain important contributors to observed variability. The present framework shows that archive-dependent temporal integration represents a first-order control that should be evaluated before invoking more complex climatic mechanisms. Apparent differences in transition duration, event sharpness, or rates of environmental change should therefore be interpreted within the context of effective temporal resolution rather than archive type alone.

5.3. Implications for Holocene Hydroclimate Reconstructions

The generalized framework also provides useful insights into the interpretation of Holocene hydroclimate reconstructions derived from multiple archive types. Regional syntheses commonly integrate speleothems, lacustrine sediments, peat sequences, marine records, and other hydroclimatic proxies to reconstruct monsoon evolution and continental moisture variability. These archives differ substantially in their dominant filtering mechanisms despite often responding to similar climatic forcing. Speleothems generally preserve relatively high temporal resolution because post-depositional diffusion is negligible following calcite precipitation, whereas lacustrine records commonly integrate catchment storage, sediment mixing, ecological response, and broader chronological uncertainty. Therefore, differences between cave and lake records at centennial timescales do not necessarily imply conflicting hydroclimate histories but may instead arise from differences in effective temporal resolution and archive response time.

The practical workflow developed in this study provides a direct means of estimating these effects directly from archive metadata. Rather than relying solely on qualitative comparisons of proxy records, effective temporal resolution can be incorporated explicitly into inter-archive comparisons to determine the temporal bandwidth over which meaningful climatic agreement should be expected. This approach offers a practical basis for improving regional hydroclimate syntheses and for identifying the timescales over which different proxy systems can be interpreted consistently. This conceptual transition from high-frequency to low-frequency signal preservation across different archive types is illustrated schematically in Figure 10.

5.4. Timescale Dependence of Proxy Agreement

Agreement among proxy records is fundamentally dependent on the temporal bandwidth preserved within individual archives (Figure 10). Increasing effective temporal integration progressively suppresses high-frequency climatic variability while preferentially preserving longer-period climate signals. Therefore, archives characterized by contrasting effective temporal resolutions are expected to diverge most strongly at annual-to-centennial timescales but converge progressively at millennial and orbital timescales. This generalized behaviour shows high-resolution archives such as ice cores and tree rings retaining much of the original high-frequency climatic variability, whereas progressively stronger temporal filtering in speleothems, lacustrine sediments, and marine sediments shifting the preserved climatic information towards longer timescales (Figure 10). This generalized bandwidth perspective complements the numerical experiments by providing an integrated conceptual view of climate-signal preservation across the principal classes of Quaternary archives.

The progressive separation of the preservation curves shows that archive comparability depends primarily on shared temporal bandwidth rather than archive identity alone. Archives with similar effective temporal resolutions are expected to preserve comparable components of climatic variability even when formed in entirely different depositional environments. Archives belonging to the same geological category may preserve very different climate signals if their effective temporal resolutions differ substantially owing to variations in accumulation rate, sampling strategy, diffusion, or post-depositional mixing. This behaviour is consistent with previous spectral investigations indicating strong dependency of recoverable climatic information on archive response functions and preserved temporal bandwidth. The present framework extends these concepts by providing a generalized metadata-based approach for estimating first-order temporal filtering without requiring archive-specific forward modelling. However, improved agreement at longer timescales should not be interpreted as evidence that all low-frequency variability is equally reliable. Centennial- and millennial-scale reconstructions are influenced by chronological uncertainty, proxy calibration, regional climatic heterogeneity, and non-stationary archive behaviour. Therefore, effective temporal resolution represents one component of a broader uncertainty framework rather than a complete description of proxy reliability.

These results suggest that palaeoclimate records should be compared within their shared temporal bandwidth rather than solely according to archive type or nominal sampling resolution. Evaluating proxy agreement within comparable temporal scales provides a more physically meaningful basis for interpreting apparent convergence and divergence among Quaternary climate records.

5.5. Implications for Proxy Synthesis and Data Assimilation

The increasing availability of regional and global palaeoclimate databases has transformed Quaternary research from individual site interpretation towards multi-proxy synthesis and climate field reconstruction. Large collaborative initiatives such as PAGES2k, Temp12k, and other global proxy compilations integrate records from diverse archive types to reconstruct spatial and temporal patterns of past climate variability. While these syntheses have substantially improved understanding of Earth's climate evolution, they also combine archives possessing markedly different temporal resolutions, sampling strategies, and archive-response characteristics.

The present framework suggests that proxy synthesis should explicitly account for effective temporal resolution in addition to chronological uncertainty and proxy calibration. Combining records with fundamentally different temporal bandwidths may suppress high-frequency climatic variability and alter the apparent timing or duration of reconstructed events. Therefore, stacked reconstructions should be regarded as bandwidth-weighted representations of past climate rather than direct averages of independent observations. The generalized relationships developed in this study (Figures 8–10) provide a practical first-order basis for implementing such bandwidth-aware comparisons. These considerations are equally relevant for palaeoclimate data assimilation, where proxy observations are combined with climate-model simulations to reconstruct past climate states. Incorporating estimates of effective temporal resolution into proxy weighting schemes offers a practical means of improving archive comparability and reducing inconsistencies arising from unequal temporal filtering.

5.6. Relationship to Proxy System Models

The generalized framework presented here is intended to complement rather than replace archive-specific Proxy System Models (PSMs). Existing forward models, including SedProxy, PRYSM, and related archive-specific approaches, explicitly simulate physical, chemical, and biological processes governing proxy formation. These models provide detailed mechanistic descriptions of individual archive systems but require substantial archive-specific parameterization and calibration. The framework developed in this study focuses on the physical processes that are common to many Quaternary archives, namely temporal integration, sampling, diffusion, and post-depositional smoothing. Rather than reproducing individual proxy records, the objective is to provide generalized first-order estimates of effective temporal resolution, climate-signal attenuation, and duration inflation using readily available archive metadata. These complementary approaches address different scientific objectives. Archive-specific Proxy System Models remain indispensable where detailed site-scale reconstruction is required, whereas the generalized framework developed here provides a rapid screening methodology for evaluating archive comparability before undertaking computationally intensive forward modelling. Therefore, the framework may assist archive selection, guide interpretation of multi-proxy datasets, and identify situations where more detailed proxy-system analyses are warranted.

5.7. Implications for Model-Data Comparison

Meaningful comparison between geological proxy records and climate-model simulations requires both datasets to represent comparable temporal bandwidths. Earth system models routinely resolve interannual to decadal variability that may not be preserved in geological archives because of temporal integration during deposition, post-depositional modification, and analytical sampling. Therefore, direct comparison between raw model output and proxy observations may exaggerate apparent disagreement by comparing fundamentally different representations of the climate system. The generalized framework provides a practical means of identifying the temporal bandwidth over which proxy observations are expected to retain climatic information. Applying archive-equivalent temporal filtering to climate-model output prior to comparison provides a more physically consistent basis for evaluating model performance. Therefore, the framework offers a methodology for improving proxy-model comparisons without replacing more sophisticated archive-specific forward models.

5.8. Limitations and Future Directions

The framework presented here is intentionally simplified and should be regarded as a first-order approximation of climate-signal preservation. Real proxy systems frequently show nonlinear responses, threshold behaviour, seasonal bias, ecological adaptation, time-varying accumulation rates, hiatuses, and archive-specific calibration uncertainties that are not explicitly represented in the generalized formulation. Effective temporal resolution may vary substantially through time within individual records owing to changes in sedimentation rate, accumulation history, or post-depositional processes. The additive representation of temporal integration adopted here also assumes that individual smoothing mechanisms contribute independently to effective temporal resolution. Although this approximation provides a practical basis for generalized archive comparison, interactions among diffusion, sediment mixing, ecological response, and analytical sampling may be considerably more complex in individual proxy systems.

Future developments should integrate the generalized framework with archive-specific Proxy System Models, Bayesian chronological approaches, and measured age-depth uncertainties to provide more comprehensive representations of climate-signal preservation. Extension of the framework to asymmetric response functions, time-dependent accumulation histories, nonlinear archive behaviour, and geographically distributed proxy networks would further improve its applicability to regional and global palaeoclimate synthesis. Application to well-characterized observational datasets will also provide opportunities for quantitative evaluation of the extent to which temporal filtering contributes to apparent disagreement among Quaternary climate records.

6. Conclusions

This study develops a generalized quantitative framework for evaluating climate-signal preservation in Quaternary palaeoclimate archives based on the common physical processes governing temporal integration. Rather than treating archive type as the primary determinant of climatic fidelity, the framework shows that effective temporal resolution, controlled by measurable properties such as accumulation rate, sampling interval, diffusion, sediment mixing, and ecological response time, provides a transferable basis for comparing heterogeneous geological archives.

Numerical experiments show that increasing temporal integration systematically attenuates abrupt climatic events, inflates apparent event duration, suppresses high-frequency variability, and redistributes climatic variance toward longer timescales. These predictable effects provide a physical explanation for many apparent differences among proxy records that respond to the same underlying climatic forcing. The representative applications to Greenland ice cores, Chinese speleothems, and North Atlantic marine sediments show that readily available archive metadata can be translated into first-order estimates of effective temporal resolution and expected climate-signal preservation without requiring detailed archive-specific forward modelling. Together with the conceptual synthesis, these representative applications indicate that archive comparability is governed primarily by shared effective temporal resolution rather than archive identity alone.

The framework has important implications for Quaternary palaeoclimate research. It provides a practical methodology for evaluating archive comparability prior to proxy interpretation, supports more robust comparison of records with contrasting temporal characteristics, and offers a physically consistent basis for multi-proxy synthesis and proxy-model comparison. Rather than replacing archive-specific Proxy System Models, the proposed methodology complements them by providing a generalized first-order screening tool that can guide archive selection, identify potential limitations arising from temporal filtering, and improve interpretation of heterogeneous palaeoclimate datasets.

Although intentionally simplified, the framework establishes a unified conceptual and quantitative basis for assessing climate-signal preservation across diverse Quaternary archives. Future developments integrating archive-specific process models, Bayesian age modelling, and time-dependent archive behaviour will extend its applicability. As palaeoclimate research increasingly relies on integrated proxy networks and large community databases, explicit consideration of archive-dependent temporal filtering will be essential for producing more consistent reconstructions of Earth's past climate variability.

Author Contributions

M.G.: Conceptualization, Methodology, Formal analysis, Investigation, Visualization, Writing—original draft, Writing—review & editing. D.B.: Supervision, writing—review and editing.

Funding

This research received no specific grant from any funding agency in the public, commercial, or not-for-profit sectors.

Institutional Review Board Statement

Not applicable.

Informed Consent Statement

Not applicable.

Data Availability Statement

No new empirical datasets were generated in this study. All numerical experiments are based on synthetic signals and analytical formulations described within the manuscript.

Acknowledgments

The authors acknowledge the broader palaeoclimate research community for developing openly accessible datasets and methodological frameworks that informed this synthesis. The authors also acknowledge DST-FST (SR/FST/ESI-107/2010) for providing the research infrastructure at the Department of Applied Geology, Dibrugarh University. We sincerely thank the Editor and the Reviewers for their careful evaluation of our manuscript and for their constructive comments and insightful suggestions. Their feedback has been invaluable in improving the scientific quality, clarity, and overall presentation of the manuscript.

Conflicts of Interest

The authors declare that they have no known competing financial interests or personal relationships that could have appeared to influence the work reported in this paper.

Use of AI and AI-assisted Technologies

During the preparation of this work, the author has used Chat GPT and Grammarly for language improvement. After using the tools, the author reviewed and edited the content as needed and take full responsibility for the content of the publication.

References

1. Bradley, R.S. *Paleoclimatology: Reconstructing climates of the Quaternary*, 2nd ed.; Elsevier Academic Press: San Diego, CA, USA, 1999; Volume 68.
2. Cronin, T.M. *Paleoclimates: Understanding Climate Change Past and Present*; Columbia University Press: New York, NY, USA, 2009.
3. Tierney, J.E.; Pausata, F.S.R.; deMenocal, P.B. Rainfall regimes of the Green Sahara. *Sci. Adv.* **2017**, *3*, e1601503. https://doi.org/10.1126/sciadv.1601503
4. Marcott, S.A.; Shakun, J.D.; Clark, P.U.; et al. A reconstruction of regional and global temperature for the past 11,300 years. *Science* **2013**, *339*, 1198–1201. https://doi.org/10.1126/science.1228026
5. Kaufman, D.; McKay, N.; Routson, C.; et al. Holocene global mean surface temperature, a multi-method reconstruction approach. *Sci. Data* **2020**, *7*, 201. https://doi.org/10.1038/s41597-020-0530-7
6. Konecky, B.L.; McKay, N.P.; Churakova (Sidorova), O.V.; et al. The Iso2k database: A global compilation of paleo-δ^{18}O and δ^{2}H records. *Earth Syst. Sci. Data* **2020**, *12*, 2261–2288. https://doi.org/10.5194/essd-12-2261-2020
7. Evans, M.N.; Lücke, L.J.; Fan, K.J.; et al. A database of databases for Common Era paleoclimate applications. *Earth Syst. Sci. Data* **2026**, *18*, 1185–1202. https://doi.org/10.5194/essd-18-1185-2026
8. Luecke, L.; Evans, M.; Zhu, F.; et al. *lluecke/dod2k*, DoD2k Version 2.0 (v2.0); Zenodo: Geneva, Switzerland, 2026. https://doi.org/10.5281/zenodo.18152672
9. Reschke, M.; Rehfeld, K.; Laepple, T. Empirical estimate of the signal content of Holocene temperature proxy records. *Clim. Past* **2019**, *15*, 521–537. https://doi.org/10.5194/cp-15-521-2019
10. Dolman, A.M.; Kunz, T.; Groeneveld, J.; et al. A spectral approach to estimating the timescale-dependent uncertainty of paleoclimate records – Part 2: Application and interpretation. *Clim. Past* **2021**, *17*, 825–841. https://doi.org/10.5194/cp-17-825-2021
11. Evans, M.N.; Tolwinski-Ward, S.E.; Thompson, D.M.; et al. Applications of proxy system modeling in high resolution paleoclimatology. *Quat. Sci. Rev.* **2013**, *76*, 16–28. https://doi.org/10.1016/j.quascirev.2013.05.024
12. Dee, S.G.; Steiger, N.J.; Emile-Geay, J.; et al. On the utility of proxy system models for estimating climate states over the common era. *J. Adv. Model. Earth Syst.* **2016**, *8*, 1164–1179. https://doi.org/10.1002/2016ms000677
13. Dolman, A.M.; Laepple, T. Sedproxy: A forward model for sediment-archived climate proxies. *Clim. Past* **2018**, *14*, 1851–1868. https://doi.org/10.5194/cp-14-1851-2018
14. Johnsen, S.J.; Clausen, H.B.; Dansgaard, W.; et al. The δ18O record along the Greenland Ice Core Project deep ice core and the problem of possible Eemian climatic instability. *J. Geophys. Res. Oceans* **1997**, *102*, 26397–26410. https://doi.org/10.1029/97jc00167
15. Fairchild, I.J.; Baker, A. *Speleothem Science*; Wiley-Blackwell: Chichester, UK, 2012. https://doi.org/10.1002/9781444361094
16. Amrhein, D.E. How large are temporal representativeness errors in paleoclimatology? *Clim. Past* **2020**, *16*, 325–340. https://doi.org/10.5194/cp-16-325-2020
17. Zuhr, A.M.; Wahl, S.; Steen-Larsen, H.C.; et al. Spatial and temporal stable water isotope data from the upper snowpack at the EastGRIP camp site, NE Greenland, sampled in summer 2018. *Earth Syst. Sci. Data* **2024**, *16*, 1861–1874. https://doi.org/10.5194/essd-16-1861-2024
18. Kunz, T.; Laepple, T. Effective spatial degrees of freedom of natural temperature variability as a function of frequency. *J. Climate* **2024**, *37*, 2505–2518. https://doi.org/10.1175/jcli-d-23-0040.1
19. Andersen, K.K.; Azuma, N.; Barnola, J.-M.; et al. High-resolution record of Northern Hemisphere climate extending into the last interglacial period. *Nature* **2004**, *431*, 147–151. https://doi.org/10.1038/nature02805
20. Rasmussen, S.O.; Andersen, K.K.; Svensson, A.M.; et al. A new Greenland ice core chronology for the last glacial termination. *J. Geophys. Res. Atmos.* **2006**, *111*, D6. https://doi.org/10.1029/2005jd006079
21. Steffensen, J.P.; Andersen, K.K.; Bigler, M.; et al. High-resolution greenland ice core data show abrupt climate change happens in few years. *Science* **2008**, *321*, 680–684. https://doi.org/10.1126/science.1157707
22. Bond, G.; Broecker, W.; Johnsen, S.; et al. Correlations between climate records from North Atlantic sediments and Greenland ice. *Nature* **1993**, *365*, 143–147. https://doi.org/10.1038/365143a0
23. Denton, G.; Alley, R.; Comer, G.; et al. The role of seasonality in abrupt climate change. *Quat. Sci. Rev.* **2005**, *24*, 1159–1182. https://doi.org/10.1016/j.quascirev.2004.12.002
24. Cheng, H.; Edwards, R.L.; Sinha, A.; et al. The Asian monsoon over the past 640,000 years and ice age terminations. *Nature* **2016**, *534*, 640–646. https://doi.org/10.1038/nature18591
25. Dee, S.G.; Russell, J.M.; Morrill, C.; et al. PRYSM v2.0: A proxy system model for lacustrine archives. *Paleoceanogr. Paleoclimatol.* **2018**, *33*, 1250–1269. https://doi.org/10.1029/2018pa003413
26. Fischer, M.J. The measurement error proxy system model: MEPSM v0.2. *Geosci. Model Dev.* **2024**, *17*, 6745–6760. https://doi.org/10.5194/gmd-17-6745-2024
27. Harper, D.; Polissar, P.; Zhang, Y.; et al. Forward modeling the alkenone paleo-CO_2 Proxy: Combining traditional approaches in a Bayesian framework. In *Goldschmidt2023 Abstracts*; The Geochemical Society & European Association of Geochemistry (EAG): Lyon, France, 2023. https://doi.org/10.7185/gold2023.18606
28. Hathorne, E.; Dolman, A.M.; Laepple, T. Assessing seasonal and inter-annual marine sediment climate proxy data. *Paleoceanogr. Paleoclimatol.* **2023**, *38*, e2023PA004649. https://doi.org/10.1029/2023pa004649
29. Wallace, E.J.; Dee, S.; Bregy, J.; et al. A proxy system modeling approach to combining tree-ring and sediment-based paleotempestological records. *Paleoceanogr. Paleoclimatol.* **2024**, *39*, e2024PA004870. https://doi.org/10.1029/2024pa004870
30. Fang, M.; Li, X. Paleoclimate data assimilation: Its motivation, progress and prospects. *Sci. China Earth Sci.* **2016**, *59*, 1817–1826. https://doi.org/10.1007/s11430-015-5432-6
31. Tierney, J.E.; King, J.; Osman, M.B.; et al. Pliocene warmth and patterns of climate change inferred from paleoclimate data assimilation. *AGU Adv.* **2025**, *6*, e2024AV001356. https://doi.org/10.1029/2024av001356
32. Zhang, H.; Li, M.; Hu, Y. Paleoclimate data assimilation: Principles and prospects. *Sci. China Earth Sci.* **2025**, *68*, 407–424. https://doi.org/10.1007/s11430-024-1439-y
33. Ning, L.; Liu, J.; Liu, Z.; et al. Progress and prospects of paleoclimate data assimilation. *Sci. China Earth Sci.* **2026**, *69*, 1605–1617. https://doi.org/10.1007/s11430-025-1810-2

34. Fang, M.; Wang, J.; Chang, H. Reconstruction of Holocene Northern Hemisphere precipitation fields using paleoclimate data assimilation. *Sci. Data* **2026**, *13*, 235. https://doi.org/10.1038/s41597-026-06551-6

35. Marshall, C.; Morrill, C.; Dee, S.; et al. Proxy System Biases partially resolve long-standing paleoclimate data-model discrepancies in Tropical East Africa. *Quat. Sci. Rev.* **2025**, *366*, 109426. https://doi.org/10.1016/j.quascirev.2025.109426

36. McPartland, M.Y.; Münch, T.; Dolman, A.M.; et al. The colors of proxy noise. *Clim. Past* **2025**, *21*, 1917–1931. https://doi.org/10.5194/cp-21-1917-2025

37. Cosentino, N.J.; Torre, G.; Lambert, F.; et al. Paleo±Dust: Quantifying uncertainty in paleo-dust deposition across archive types. *Earth Syst. Sci. Data* **2024**, *16*, 941–959. https://doi.org/10.5194/essd-16-941-2024

38. Govin, A.; Braconnot, P.; Capron, E.; et al. Persistent influence of ice sheet melting on high northern latitude climate during the early Last Interglacial. *Clim. Past* **2012**, *8*, 483–507. https://doi.org/10.5194/cp-8-483-2012

39. Trauth, M.H.; Sarnthein, M.; Arnold, M. Bioturbational mixing depth and carbon flux at the seafloor. *Paleoceanography* **1997**, *12*, 517–526. https://doi.org/10.1029/97pa00722